J. Chem. Sci. Vol. 124, No. 1, January 2012, pp. 261–269.

Structure and transport properties of LiF–BeF_2 mixtures: Comparison of rigid and polarizable ion potentials[#]

B SHADRACK JABES, MANISH AGARWAL and CHARUSITA CHAKRAVARTY*
Department of Chemistry, Indian Institute of Technology Delhi, New Delhi 110 016, India
e-mail: charus@chemistry.iitd.ernet.in

Abstract. Molecular dynamics simulations are performed to study the structure and dynamics of the LiF–BeF_2 system over a range of compositions using the transferable rigid-ion model (TRIM). The densities obtained with the TRIM potential are approximately 17–20% lower than the experimental values while polarizable ion models (PIM) give densities within 5% of the experimental value. The TRIM and PIM potentials give essentially identical radial distribution functions (RDFs) for Li–F and Be–F ion pairs though the Be–Be pair correlations differ significantly and reflect the corresponding density differences. The variation in the radial distribution functions with concentration, particularly the anion–anion pair correlation function, reflects the reorganization of the fluoride ions as the addition of BeF_2 in the mixture promotes the formation of the tetrahedral fluoroberyllate network. Along the 67 mol% LiF isopleth, diffusivities and Nernst–Einstein ionic conductivities from simulations using the PIM and TRIM potentials are in good agreement for temperatures up to 925 K. The viscosity data using the PIM model is also found to be in good agreement with the TRIM results presented here along the 873 K isotherm for compositions ranging from 0 to 50 mol% BeF_2. The main conclusion from this study is that the non-polarizable, TRIM provides reasonable results for the structural correlations and transport properties of the LiF–BeF_2 system in comparison with first-principles-based, PIM.

Keywords. Molten salts; ionic liquids; molecular dynamics; transport properties; ionic conductivity; viscosity.

1. Introduction

Ionic liquids are liquids with non-zero electrical conductivity where the charge carrying entities are based on atomic or molecular ions. Examples of such ionic liquids are molten oxides and halides of many elements which may be thought of as a multi-component mixture of atoms with very different electronegativities. If the electronegativity difference is large, Coulombic interactions dominate structure, as in alkali halides, and the corresponding molten salts can be regarded as simple liquids.[1] As the electronegativity difference decreases, however, local anisotropic or "covalent" interactions result in the formation of complex, network-forming liquids e.g., molten BeF_2, SiO_2, or $AlCl_3$. Further decrease in electronegativity or increase in covalency results in the formation of chains or ribbons, as in the case of $BeCl_2$ or GeS_2. The complex interplay of relative electronegativities and polarizabilities results in a diversity of liquid state structures, anomalous properties and polyamorphic phases, many of which have significant technological applications.[2,3]

Many of the AB_2 ionic melts form three-dimensional, locally tetrahedral networks similar to the hydrogen-bonded network of water. Examples of such ionic melts include one-component systems, such as SiO_2,[4–14] BeF_2,[15–22] $ZnCl_2$[23–25] and GeO_2,[26,27] and binary mixtures, such as GeO_2 $-SiO_2$, Si_xTe_{100-x}, Ge_xTe_{100-x} and LiF–BeF_2. Chemical bonding in such systems may be considered to be partially ionic and partially covalent in origin, with the degree of covalency related to the ionic polarizability. Depending on the nature of bonding, the bias towards local tetrahedral order around the cation may be explained on the basis of local, anisotropic covalent bonding or in terms of steric effects associated with packing of ions with specific cation-to-anion radius ratios. The transport properties of such ionic liquids are of importance in many applications. For example, mobility of molten silicates and aluminosilicates is of geophysical importance since it determines mass and heat transport in the earth's mantle. The LiF–BeF_2 system is of importance as a solvent for actinide ions in the molten salt reactor and as a heat exchanger or blanket material in proposed breeder and fusion reactors. The most important transport properties in the context of ionic liquids are the diffusivity, the ionic conductivity and the viscosity which measure the response of a system to perturbation

[#]Dedicated to Prof. N Sathyamurthy on his 60th birthday
*For correspondence

due to mass gradients, electric fields or velocity gradients, respectively. These transport properties are alternative measures of molecular mobility, with the diffusivity being a single-particle property while ionic conductivity and viscosity are collective transport properties.

The structural and transport properties of LiF–BeF_2 mixtures show interesting variations with composition. At ambient pressure conditions, liquid BeF_2 forms a tetrahedrally coordinated network structure. When a low concentration of liquid BeF_2 is combined with LiF, the mixture behaves as a well dissociated ionic melt consisting of BeF_4^{2-}, Li^+ and F^- ions. As the BeF_2 concentration increases, the viscosity shows a very substantial increase with the progressive formation of a fluoroberyllate network. In the same concentration range, the motion of the Li^+ ions begins to dominate the conductivity and the Li^+ diffusion coeficient and conductivity exhibit a remarkable decoupling from the viscosity, with a corresponding breakdown of the Stokes–Einsteins relation.[22,28] This is a phenomenon of great technological interest as it is associated with formation of good ionic conductors in nearly rigid materials with high viscosity. Therefore by varying the composition of BeF_2 in LiF, one expects to see a wide range of fluidity[22] and network formation. This system therefore is an excellent one for examining the relationships between dynamic properties like diffusivities, ionic conductivities, viscosities and liquid state structure using molecular dynamics simulations.

In order to map out the relationships between liquid state structure and dynamical properties over a wide range of temperatures and compositions for ionic melts, it is necessary to have efficient potential energy models. While first principles approach is the most accurate,[29] they are also computationally expensive. A recent approach for molten salt systems is to use force-matching approaches to fit parametric potentials to data from first principles simulations. In the case of tetrahedral, network-forming liquids, it is found that polarizable ion models (PIM) in which the ions interact through pairwise additive Born-Mayer functions, augmented by a description of anion polarization using a (dipolar) PIM, provide a very adequate description over a wide degree of covalency.[30] In the PIM, the anion polarizability controls the MXM angle via the presence of induced dipole moments on bridging anions which act to screen the repulsive Coulombic interaction between cations. Low anion polarizabilities (0–10 atomic units) are associated with the tetrahedral ionic melts, most notably, SiO_2, BeF_2 and GeO_2. Rigid-ion potentials set the polarizability to zero and model the interactions using a combination of long-range Coulombic and short-range repulsion-dispersion terms.[31]

Molecular dynamics simulations of liquid silica and beryllium fluoride are performed using rigid ion model potentials, have revealed some interesting features of the relationships between structure, transport and thermodynamic properties of network-forming ionic melts.[32–34] The ionic conductivity (σ), shear viscosity (η) and ionic self-diffusivities (D) were computed over a fairly wide range of temperatures and densities. The Stokes–Einstein relation was shown to hold over the entire range of state points, though the effective hydrodynamic radius showed small variations due to thermal fluctuations, compression, and local tetrahedral order. The Nernst–Einstein relation was shown to break down due to significant network-formation in the anomalous regime leading to a breakdown of this relationship. The scaling behaviour of the diffusivity and viscosity with excess entropy were shown to hold over a fairly wide temperature range and to break down only with onset of cooperativity in the diffusion dynamics. A recent study also validates the entropy scaling relationships for the diffusivity of an idealized 2:1 model molten salt.[35]

The motivation for the current study was to examine the reliability of the rigid-ion potentials, in comparison with the first principles parameterized polarizable-ion potential, with regard to mapping out structure, entropy and mobility relationships of ionic melts. The LiF–BeF_2 system was chosen since it displays anomalous, tetrahedral liquid behaviour as a function of temperature, pressure and composition. Polarizability effects are least for BeF_2 among the tetrahedral ionic melts and therefore a rigid-ion potential may be expected to be most physically reasonable for this system. The transferable rigid-ion model (TRIM) for this system is written as a sum of Coulombic interactions and Born-Mayer repulsion terms.[36–38] Initial comparisons of the PIM and TRIM models for BeF_2 compared the equations of state and the diffusivities along the 1.96 g cm^{-3} density, which corresponds to the BeF_2 density at ambient pressure[20]. Structural and transport properties are available for the LiF–BeF_2 system at a restricted set of state points and compositions using the polarizable ion (PIM) potential but are not compared with the rigid-ion results.[21,39] In this paper, we present a more extensive study of structure and dynamis of the LiF–BeF_2 system over a range of compositions using the rigid-ion model, allowing us to perform a more detailed comparison of the rigid-ion and polarizable ion models, including collective transport properties (viscosity and conductivity). Computational details are summarized in section 2. Results

and conclusions are presented in sections 3 and 4, respectively.

2. Computational details

2.1 *Potential energy surface*

The TRIM potential characterises each ionic species α by parameters corresponding to ionic charge (z_α), characteristic size parameter (σ_α) and number of valence electrons (n_α). The TRIM potential is pair-additive with the pair interaction between two ions of species α and β separated by a distance r written as a sum of Coulombic and Born–Mayer repulsion terms in the form

$$\phi_{TRIM}(r) = \frac{z_\alpha z_\beta e^2}{4\pi\epsilon_0 r} + \left(1 + \frac{z_\alpha}{n_\alpha} + \frac{z_\beta}{n_\beta}\right) \times b \exp\left[\frac{1}{\rho}(\sigma_\alpha + \sigma_\beta - r)\right]. \quad (1)$$

The repulsion parameter b and the softness parameter ρ are assumed to be the same for all the six types of pair interactions in $LiBeF_3$. The values of TRIM parameters are given in table 1.

2.2 *Molecular dynamics*

Molecular dynamics simulation of a system of Li, Be and F ions with nearly 450 atoms were carried out in the NVT ensemble under cubic periodic conditions using the DL_POLY software package.[40] The leapfrog algorithm with a time step of 1fs was used to integrate the equation of motion. Ewald summation method was used to account for long range electrostatic interaction. The Berendson thermostat with a time constant of $\tau_B = 10$ ps for highly diffusive regimes and $\tau_B = 200$ ps for highly viscous regimes was used in order to maintain desired temperature for the production runs. For the production runs to estimate dynamical properties, NVT runs were used with thermostat time constant choosen to be greater than the correlation time of the autocorrelation functions relevant for estimation of dynamic quantities to minimize perturbation of the intrinsic dynamics of the system.

Table 1. TRIM potential parameters for $LiBeF_3$ taken from[37]: σ_α, z_α and n_α are the ionic sizes, charges and the number of valence shell electrons of the different species α, respectively. The values of the softness parameter, ρ is 0.290(Å) and the repulsion parameter, b is 2.736 (kcal mol^{-1}).

α	Li	Be	F
σ_α(Å)	0.925	0.938	1.237
z_α	+1	+2	−1
n_α	2	2	8

The different compositions of the ($LiF–BeF_2$) system studied in this work are listed in table 2, together with the number of atoms of each type. The initial configuration for each composition was prepared by placing the appropriate number of atoms randomly without any overlaps in a cubical box using the PACKMOL software.[41] The system thus obtained was heated gradually using short molecular dynamics (MD) runs of 0.4 ns with temperature changing from 2000 K to 3000 K in steps of 50 K each. This was followed by gradual cooling of the melt, using 0.1 ns MD simulations with temperature changing from 3000 K to 700 K in steps of 10 K each. Heating and cooling were carried out using NPT simulations at zero pressure with a barostat time constant of 1ps. In order to obtain static and dynamic properties as a function of temperature, the system equilibration and production runs were performed at eleven temperatures in the 775 K to 1700 K range along isopleths corresponding to ten different compositions. At these state points equilibration runs of 5–8 ns were carried out in the NPT ensemble at zero pressure. Once an equilibrium volume was obtained, the barostat was switched off and canonical ensemble production runs of 8–16 ns were performed. We note that as the mole fraction of BeF_2 increases in the mixture, equilibration becomes much slower because the viscosity increases very significantly accompanied by a decrease in diffusivity and ionic conductivity. We have reported only those state points and compositions for which reliable equilibrium averages could be obtained with 16 ns runlengths.

2.3 *Self-diffusivity*

Self-diffusivities were evaluated using the Einstein relation:

$$D_\alpha = \lim_{t\to\infty} \frac{\langle|\delta r_i(t)|^2\rangle}{6t}, \quad (2)$$

where $\delta r_i(t)$ is the displacement of individual ion i. Note that the computation of the particle displacements must be appropriately unfolded to compensate for periodic boundary conditions. Configurations were dumped every 0.5 ps in order to estimate the mean square displacements as a function of time. In order to estimate error bars, each trajectory was split into 8 non-overlapping subtrajectories and the diffusivities for each sub-trajectory were used to estimate the errors.

Table 2. Simulation cell size and equilibrium densities for LiF–BeF_2 mixtures of different composition.

LiF–BeF_2 (mol%)	N_{Li}	N_{Be}	N_F	N_{total}	ρ (g/cm^3) TRIM (P = 0atm, 1500 K)	ρ (g/cm^3) TRIM (P = 1atm, 1123 K)	ρ[47] (g/cm^3) Exp (P = 1 atm, 1123 K)
0–100	0	150	300	450	...	...	1.960
10–90	15	135	285	435	1.559	1.568	1.909
20–80	32	128	288	448	1.518		
25–75	40	120	280	440	...	1.528	1.889
30–70	48	112	272	432	1.525		
40–60	68	102	272	442	1.460		
50–50	90	90	270	450	1.486	1.503	1.873
60–40	108	72	252	432	1.452		
70–30	133	57	247	437	1.403		
80–20	160	40	240	440	1.410		
90–10	189	21	231	441	1.369		

2.4 *Shear viscosity*

Using the Green–Kubo relationship, the shear viscosity η was calculated from the time integral of the autocorrelation function of an off-diagonal element of the pressure tensor, given by[42]

$$\eta = \frac{V}{k_B T}\int_0^\infty \langle P_{\gamma\delta}(0)P_{\gamma\delta}(t)\rangle dt. \tag{3}$$

The elements of the pressure tensor, $P_{\gamma\delta}$, denote the force acting along direction γ on a unit surface perpendicular to the direction δ, where γ and δ are the cartesian directions x, y or z. The instantaneous value of the pressure tensor component $P_{\gamma\delta}$ at time t is given by

$$P_{\gamma\delta}(t) = \left\langle \frac{1}{V}\sum_{i=1}^{N} m_i v_{i\gamma} v_{i\delta} + \sum_{i=1}^{N}\sum_{j>i}^{N} f_{\gamma ij}(r_{i\delta} - r_{j\delta}) \right\rangle, \tag{4}$$

where V is the system volume, $v_{i\gamma}$ and $r_{i\gamma}$ are the velocity and position along direction γ of the i^{th} atom having mass m_i and $f_{\gamma ij}$ is the force between atoms i and j along direction γ. Since the potential energy surface is pair additive, therefore the pressure tensor will be symmetric $P_{xy} = P_{yx}$.[43] To get better statistics, the pressure autocorrelation function is averaged over the three independent off-diagonal components, namely P_{xy}, P_{yz} and P_{zx}. The periodic boundary condition need not be explicitly considered when evaluating the viscosity using the Green–Kubo relation. We found it necessary to dump the pressure tensor at every time step (1 fs) for obtaining an accurate estimation of the autocorrelation function. The integral must be computed over a time period sufficiently long that a stable plateau is obtained. The time taken for the integral to reach the plateau value can be used as an approximate measure for the estimation of correlation time.[43,44] The running integral of the off-diagonal pressure autocorrelation function (ACF), obtained from equation 3 is plotted as a function of time for several state points in figure 1. A stable plateau value is typically obtained within 10 ps at high temperatures for highly diffusive compositions while correlation times of the order of 200 ps are observed at low temperatures in the highly viscous composition regimes. The computation parameters that are essential for estimating the viscosity are as follows: (i) t_d is the total length of simulation; (ii) t_w is the length of the time window over which the integral of the ACF is performed and (iii) t_s is the time difference between successive windows each of length t_w. The error associated with the terminal value of the integral of the plateau region was estimated by dividing the 15 ns trajectory into non-overlaping 3 ns

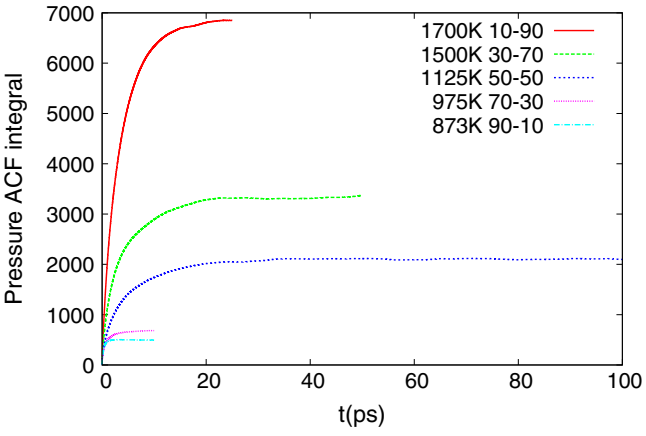

Figure 1. Running integral of the pressure autocorrelation function for different state points in the temperature–composition. Temperature is given in (K) and composition is given in (mol%).

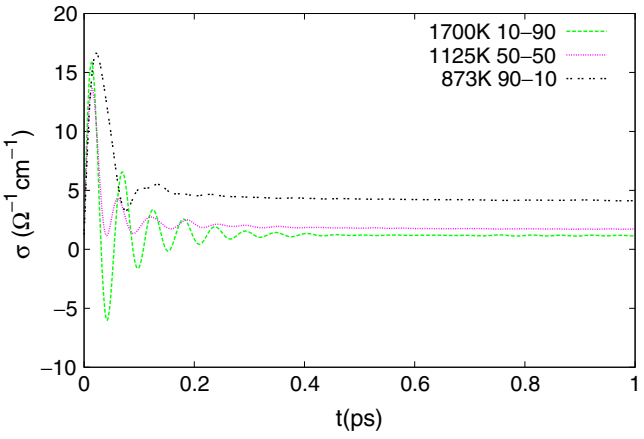

Figure 2. Running integral of the charge flux autocorrelation function for different state points in the temperature–composition plane for LiF–BeF_2 mixture. The oscillatory amplitute about the plateau value of integral is small in comparison to the actual average value.

sub-trajectories. For a given sub-trajectory, the ACF is obtained by averaging over all associated windows.

2.5 *Ionic conductivity*

The Green–Kubo relation for the ionic conductivity σ is defined as:[45]

$$\sigma = \frac{1}{3Vk_BT}\int_0^\infty \langle \mathbf{j}(t)\cdot\mathbf{j}(0)\rangle dt, \qquad (5)$$

where V and T are the volume and temperature of the system, respectively and the charge-flux vector $\mathbf{j}(t)$ is defined by

$$\mathbf{j}(t) = \sum_{i=1}^{n} z_i e v_i(t), \qquad (6)$$

where $z_i e$ and v_i are the charge and velocity of atom i, respectively. The charge flux was stored at every time step for 15×10^6 consecutive steps. The correlation times for the charge flux autocorrelation function vary from about <2 ps for high temperature, highly diffusive compositions to about <10 ps for low temperature, highly viscous composition regimes (see figure 2). The oscillations about the plateau value of the integral were much less than 3 % for most state points. Such sinusoidal oscillations can be related to the infrared spectral frequencies.[46] Ionic conductivity, as estimated from the Green–Kubo relation, is a collective property of the liquid in contrast to a single-particle property, such as the diffusivity. If, however, collective effects are small, then the Nernst–Einstein equation can be used to estimate the ionic conductivity from the ionic diffusivities, using the relation:

$$\lambda^{NE} = \frac{\beta e^2}{V}(\rho_{Be}q_{Be}^2 D_{Be} + \rho_{Li}q_{Li}^2 D_{Li} + \rho_F q_F^2 D_F), \quad (7)$$

where ρ_α is the number density of species α.

3. Results

3.1 *Equation of state and radial distribution functions*

The original comparisons of the transferable rigid ion model (TRIM) and the polarizable ion model (PIM) for BeF_2 suggested that at a given density and temperature, the equilibrium pressure was much lower for the polarizable ion model than for the rigid-ion model. This is consistent with lower densities for the rigid-ion model under isothermal–isobaric condition. The densities for the PIM potential were reported to be within 5% of the experimental values. In table 3, we show the densities

Table 3. Summary of computation parameters for Green–Kubo estimation of ionic conductivity and viscosity: The total length of simulation performed is t_d;The length of the time window is t_w over which the ACF integral are evaluated; The differnece between the origins of successive time window is t_s.

	t_d	T(K)	LiF–BeF_2(mol%)	t_w	t_s=Δ_{dump}
η	15ns	1700	10−90 to 90−10	25ps−2.5ps	1fs
		1500	10−90 to 90−10	80ps−2.5ps	
		1200	30−70 to 90−10	150ps−10ps	
		1175	30−70 to 90−10	200ps−10ps	
		1125	30−70 to 90−10	200ps−10ps	
		1075	40−60 to 90−10	150ps−10ps	
		1025	50−50 to 90−10	100ps−10ps	
		975	50−50 to 90−10	100ps−10ps	
		925	50−50 to 90−10	100ps−10ps	
		873	50−50 to 90−10	200ps−10ps	
		775	50−50 to 90−10	200ps−10ps	
σ	15ns			10ps	1fs

for different compositions under zero pressure conditions at 1500 K. In order to compare with experiment, for selected compositions, we also show the densities at 1 atm pressure along the 1123 K isotherm. For the compositions where experimental data is available, it is evident that densities obtained with the TRIM potential are approximately 17–20% lower than the experimental values. In view of this large difference in densities, it is interesting that the TRIM potential model is able to reproduce the radial distribution function (RDF) for Li–F and Be–F ion pairs obtained using the polarizable potential model, as shown in figure 3 for LiF–BeF_2 mixture containing 67% LiF. The Be–Be radial distribution functions for the polarizable and rigid-ion models is, however, distinctly different and shows the closer spacing of the peaks in the RDF consistent with the higher density of the polarizable model. The cation-anion pair correlation functions, presumably dominated by the short-range Born–Mayer repulsions in the neighbourhood of the first peak in $g(r)$, are clearly very similar for the rigid and polarizable ion models. The polarization effects presumably reduce the effective charge on the ions and result in more compact cation-cation pair distribution functions.

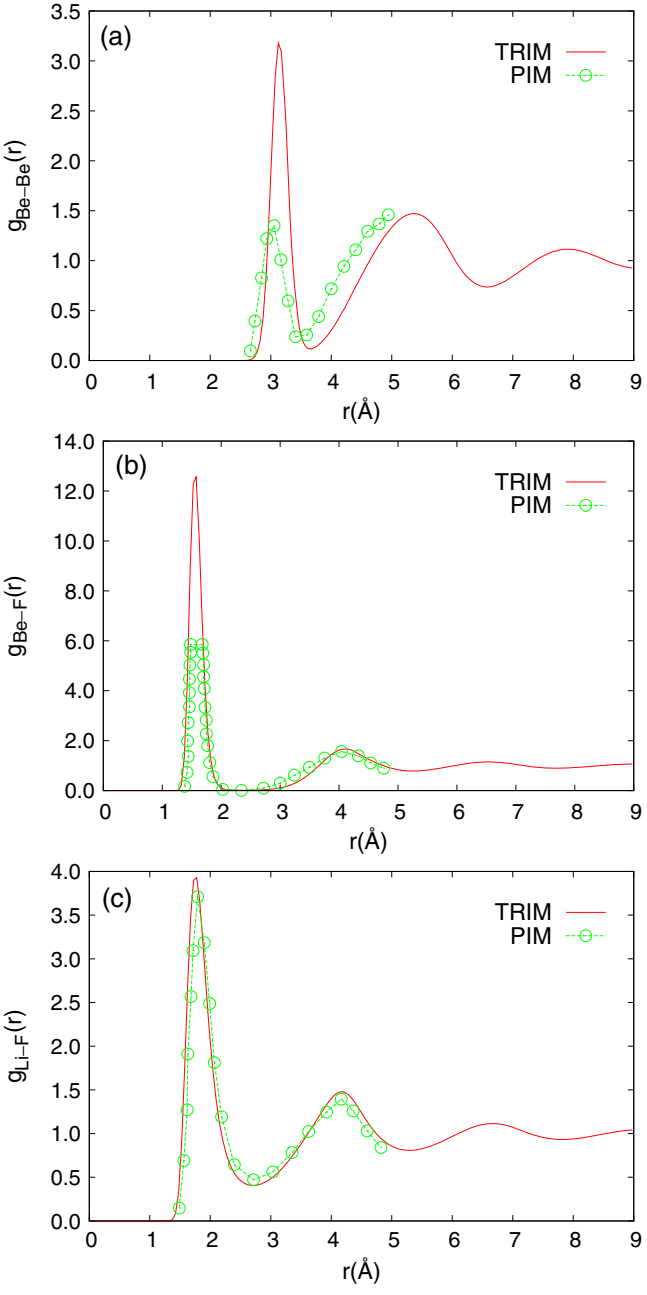

Figure 3. Comparison of radial distribution function, $g_{\alpha\beta}$, between TRIM and PIM for LiF–BeF_2 mixture at 873 K (67–33).[21]

The radial distribution function for each distinct pair at 1200 K is shown in figure 4 for several different compositions. The cation-anion correlation functions ($g_{Li-F}(r)$ and $g_{Be-F}(r)$) show very little variation with composition. In contrast, the cation-cation pair correlation functions ($g_{Li-Li}(r)$ and $g_{Be-Be}(r)$) show a dramatic change in the height of the first peak once the mole percent of BeF_2 exceeds 70%. Thus for the BeF_2 rich compositions with high viscosity, the fluoroberyllate network formation promotes the correlation between Be^{2+} cations. Therefore at higher concentration of BeF_2, the Li ions are almost left free to diffuse around the fluoroberyllate network. The clustering of beryllium cations as a consequence of the formation of the fluoroberyllate network formation, results in an effective increase in spatial correlations between lithium atoms excluded from the network. While the cation-cation pair correlation functions show changes in peak heights with concentration, the anion-anion correlation function shows striking, concentration-dependent changes in peak locations, widths and heights which must reflect the reorganization of the fluoride ions as the addition of Be^{2+} cations promotes the formation of the fluoroberyllate network. The sharpening of the first peak of $g_{F-F}(r)$ as the mol% of BeF_2 increases reflects the formation of the compact BeF_4^{2-} anions.

3.2 *Diffusivity*

Figure 5 shows diffusivities of the three ionic species in the LiF–BeF_2 system along the 67% LiF isopleth for temperatures ranging from 775 K to 1200 K using both the rigid-ion (TRIM) and polarizable ion (PIM) potentials. The polarizable ion results, taken from[21], are available only up to a temperature of 775 K to 925 K. The close agreement between the TRIM and PIM potentials for the diffusivities of each ionic species is specially remarkable given the relatively large difference in the densities obtained with the polarizable

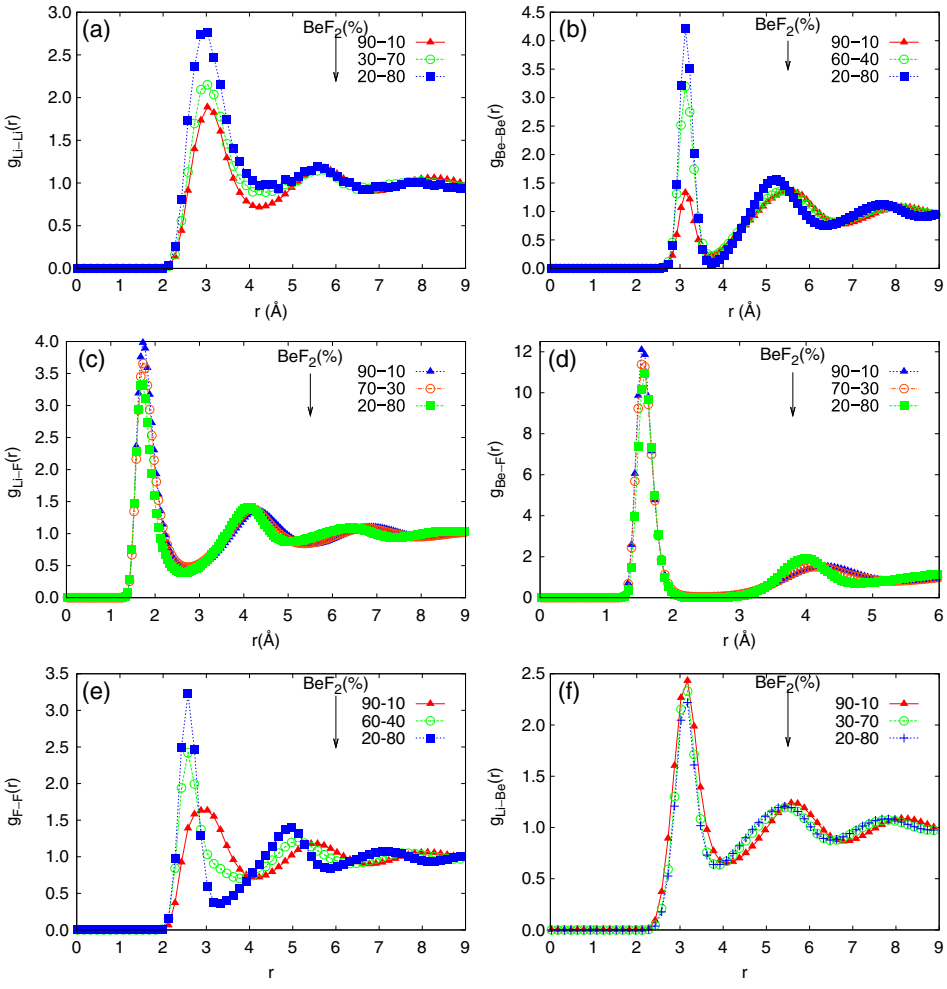

Figure 4. Radial distribution function, $g_{\alpha\beta}$, between ion species α and β for LiF–BeF_2 mixtures of different composition at 1200 K. The arrow represents the increasing concentration of BeF_2 in mol (%).

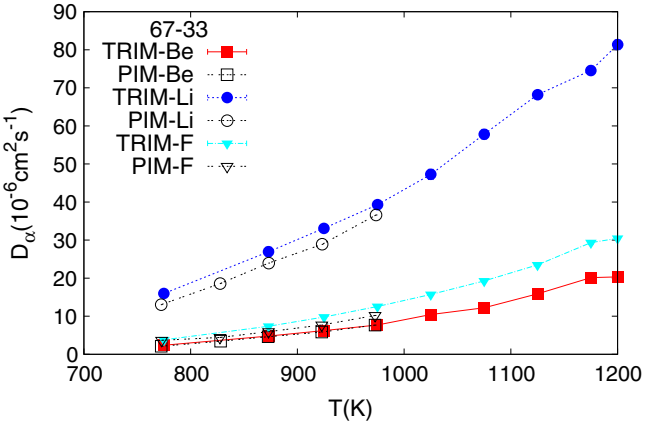

Figure 5. Behaviour of cation and anionic self diffusion coefficient (D_α) as a function of temperature calculated using TRIM are compared with PIM[21] for the LiF–BeF_2 system at (67–33). The error bars estimated using block averaging is less than 2% for diffusivities of ions.

and non-polarizable ion potentials. The results for the RDFs, together with our studies of excess entropy scaling of transport properties of ionic melts,[34] suggest that this must be due the fact that the cation-anion RDFs are very similar for the TRIM and PIM potentials and must play a crucial role in controlling diffusivity. It is evident that the most mobile species is Li^{2+}, while the F^- and Be^{2+} ions have a very similar diffusion.

3.3 *Viscosity*

Figure 6 compares the viscosity obtained using the TRIM and PIM models as a function of composition along the 873 K isotherms at zero pressure. Also shown are the TRIM results for the viscosity along the 1175 K isotherm. As in the case of the diffusivity, the agreement between polarizable and rigid-ion results for the

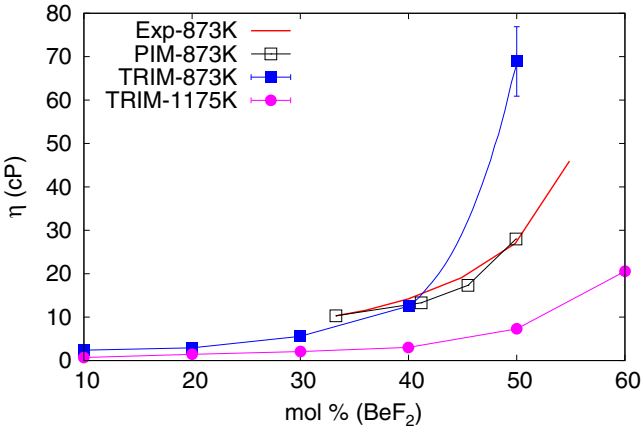

Figure 6. Behaviour of viscosity as a function composition of BeF_2 in (mol%) calculated using TRIM are compared with experiment and PIM for the LiF–BeF_2 system at 873 K and 1175 K isotherms.[21] The error bars estimated using block averaging is less than 11% for viscosity.

diffusivity is very good, except at 873K and at a composition corresponding to 50 mol% BeF_2, the difference between the two models is 41 cP.

3.4 *Conductivity*

Figure 7 compares the Nernst–Einstein estimates for the ionic conducivity obtained using the polarizable and rigid-ion models along the 67 LiF mol% isopleth. We also show the ionic conductivity using the Green–Kubo formulation. Below 950 K, comparison of the Green–Kubo and the Nernst–Einstein results for the conductivity are in good agreement for the TRIM potential. The TRIM results also are in good agreement with the PIM results and with experiment.[21] We were not able to find experimental conductivity data above 950 K for

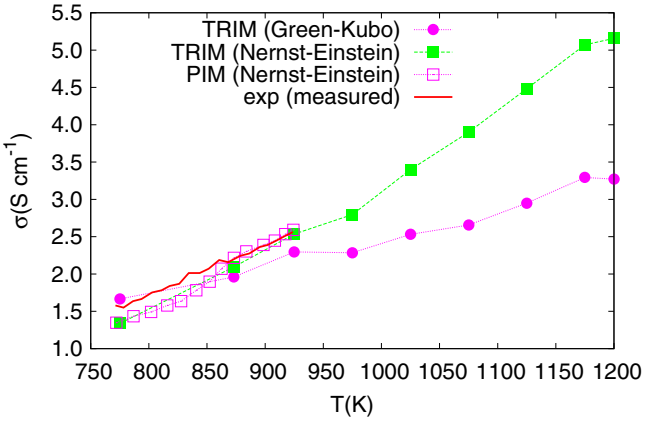

Figure 7. Behaviour of ionic conductivity as a function temperature calculated using TRIM are compared with experiment and PIM for the LiF–BeF_2 system at (67–33).[21]

this system. Our results also show that the Nernst–Einstein and Green–Kubo estimates for ionic conductivity diverge at higher temperatures.

4. Conclusions

In this paper, we present molecular dynamics study of structure and dynamics of the LiF–BeF_2 system over a range of compositions using the rigid-ion model, allowing us to perform a detailed comparison of the rigid-ion (TRIM) and polarizable ion (PIM) models. The densities obtained with the TRIM potential are approximately 17–20% lower than the experimental values; in comparison, the polarizable ion models give densities within 5% of the experimental value. Despite this large difference in densities, the TRIM and PIM potentials give essentially identical radial distribution functions (RDFs) for Li–F and Be–F ion pairs. The Be–Be pair correlation functions are, however, different for the rigid-ion and polarizable ion models and reflect the corresponding density differences.

Using the TRIM potential, we have studied the variation in the radial distribution functions with concentration. The cation–anion correlation functions ($g_{Li-F}(r)$ and $g_{Be-F}(r)$) show very little variation with composition. In contrast, the cation–cation pair correlation functions ($g_{Li-Li}(r)$ and $g_{Be-Be}(r)$) show a dramatic change in the height of the first peak once the mole percent of BeF_2 exceeds 70%. Composition-dependent variations are most striking in the anion–anion correlation function and reflect the reorganization of the fluroide ions as the addition of BeF_2 promotes the formation of the fluoroberyllate network.

For a single isopleth (67 mol% LiF) diffusivities and ionic conductivities are available using the polarizable ion model for temperatures up to 925 K. The TRIM potential gives good agreement with diffusivities obtained using the PIM model. The results for the RDFs, together with our studies of excess entropy scaling of transport properties of ionic melts,[33,34] suggest that this must be due to the fact that the cation–anion RDFs are very similar for the TRIM and PIM potentials and must play a crucial role in controlling diffusivity. From the TRIM simulations, we can show that the Nernst–Einstein approximation is valid for this system at temperatures below 1000 K, allowing an estimate of the ionic conductivity from the ionic diffusivities. We also show that in this regime, our results for ionic conductivity agree well with polarizable ion estimates based on the Nernst–Einstein relation. The viscosity data using the PIM model is found along the 873 K isotherm for compositions ranging from 0 to 50 mol%

BeF_2. Within this concentration range, the viscosities from the PIM and TRIM models agree.

To summarize, the main conclusion from this study is that the non-polarizable, transferable rigid ion model (TRIM) provides reliable results for structural correlations and transport properties of the LiF–BeF_2 system in comparison with first-principles-based, polarizable ion models (PIM). Therefore, such rigid models can be used to provide semiquantitatively accurate results for transport properties of such binary ionic melts over a wide range of state points and composition. This should facilitate an understanding of the effect of structure and composition on diffusivity–viscosity–conductivity relationships of ionic melts that are important for practical applications.

Acknowledgements

The author CC thanks the Department of Science and Technology, New Delhi for financial support. BSJ thanks the Indian Institute of Technology, New Delhi for the award of Junior and Senior Research Fellowships, respectively. The authors would like to thank Abir Ganguly for help in the initial stages of the work.

References

1. Hansen J P and McDonald I R 2006 *Theory of simple liquids* (Amsterdam: Elsevier Academic Press)
2. Madden P A and Wilson M 2000 *J. Phys-Cond. Matt.* **12** A95
3. McMillan P F, Wilson M, Wilding M C, Daisenberger D, Mezouar M and Greaves G N 2007 *J. Phys-Cond. Matt.* **19** 415101
4. Scala A, Starr F W, Nave E L, Sciortino F and Stanley H E 2000 *Nature* **406** 166
5. Saika-Voivod I, Poole P H and Sciortino F 2001 *Nature* **412** 514
6. Saika-Voivod I, Sciortino F and Poole P H 2004 *Phys. Rev. E.* **69** 041503
7. Shell M S, Debenedetti P G and Panagiotopoulos A Z 2002 *Phys. Rev. E.* **66** 011202
8. Wilson M, Madden P A, Hemmati M and Angell C A 1996 *Phys. Rev. Lett.* **77**, 4023
9. Hemmati M and Angell C A 1997 *J. Non-Cryst. Solids* **217** 236
10. Poole P H, Hemmati M and Angell C A 1997 *Phys. Rev. Lett.* **79** 2281
11. Saika-Voivod I, Sciortino F and Poole P H 2000 *Phys. Rev. E.* **63** 011202
12. Ford M H, Auerbach S M and Monson P A 2004 *J. Chem. Phys.* **121** 8415
13. Horbach J and Kob W 1999 *Phys. Rev. B* **60** 3169
14. Voigtmann T and Horbach J 2008 *J. Phys-Cond. Matt.* **20** 244117
15. Wright A C, Clare A G, Etherington G, Sinclair R N, Brawer S A and Weber M J 1989 *J. Non-Cryst. Solids* **111** 139
16. Takada A, Richet P, Catlow C R A and Price G D 2007 *J. Non-Cryst. Solids* **353** 1892
17. Hemmati M, Moyinihan C T and Angell C A 2001 *J. Chem. Phys.* **115** 6663
18. Brawer S A 1980 *Phys. Rev. Lett.* **46** 778
19. vander Meer J P M and Konings R J M 2007 *J. Nucl. Mater.* **360** 16
20. Heaton R J, Brookes R, Madden P A, Salanne M, Simon C and Turq P 2006 *J. Phys. Chem. B* **110** 11454
21. Salanne M, Simon C, Turq P, Heaton R J and Madden P A 2006 *J. Phys. Chem. B* **110** 11461
22. Salanne M, Simon C, Turq P and Madden P A 2007 *J. Phys. Chem. B* **111** 4678
23. Wilson M and Madden P A 1998 *Phys. Rev. Lett.* **80** 532
24. Wilson M, Sharma B K and Massobrio C 2008 *J. Chem. Phys.* **128**, 244505
25. Sharma B K and Wilson M 2008 *J. Phys-Cond. Matt.* **20** 244123
26. Micoulaut M, Cormier L and Henderson G S 2006 *J. Phys-Cond. Matt.* **18** R753
27. Shanavas K V, Garg N and Sharma S M 2006 *Phys. Rev. B* **73** 094120
28. Angell C A, Imrie C T and Ingram M D 1998 *Polym. Int.* **47** 9
29. Madden P A, Heaton R, Aguado A and Jahn S 2006 *J. Mol. Struc-Theochem.* **771** 9
30. Wilson M and Salmon P S 2009 *Phys. Rev. Lett.* **103** 157801
31. Tosi M P and Fumi F G 1964 *J. Phys. Chem. Solids.* **25** 45
32. Agarwal M and Chakravarty C 2009 *Phys. Rev. E.* **79** 030202
33. Agarwal M, Ganguly A and Chakravarty C 2009 *J. Phys. Chem. B* **113** 15284
34. Agarwal M, Singh M, Jabes B S and Chakravarty C 2011 *J. Chem. Phys.* **134**, article no. 014502
35. Armstrong J A and Ballone P 2011 *J. Phys. Chem. B* **115** 4927
36. Woodcock L V, Angell C A and Cheeseman P 1976 *J. Chem. Phys.* **65** 1565
37. Busing W R 1972 *J. Chem. Phys.* **57** 3008
38. Rahman A, Fowler R H and Narten A H 1972 *J. Chem. Phys.* **57** 3010
39. Salanne M, Simon C, Turq P and Madden P A 2007 *Cr Chim.* **10** 1131
40. Smith W, Yong C W and Rodger P M 2002 *Mol. Simulat.* **28** 385
41. Martinez L, Andrade R, Birgin E G and Martnez J M 2009 *J. Comp. Chem.* **30** 2157
42. Allen M D and Tildesley D J 1986 *Computer simulation of liquids* (Oxford: Clarendon Press, Oxford)
43. Rappaport D C 1998 *The art of molecular dynamics simulation* (Cambridge: Cambridge University Press)
44. Frenkel D and Smit B 2002 *Understanding molecular simulation: from algorithms to applications* (London: Academic Press)
45. Hansen J P and McDonald I R 1986 *Theory of simple liquids* (London: Academic Press)
46. Agarwal M and Chakravarty C 2009 *J. Chem. Sci.* **121** 913
47. Cantor S, Ward W T and Moynthan C T 1969 *J. Chem. Phys.* **50** 2874